Stability of cylindrical vesicles under axial tension

Dirk Jan Bukman,[1,2,*] Jian Hua Yao,[1] and Michael Wortis[1]
[1]*Department of Physics, Simon Fraser University, Burnaby, British Columbia, Canada V5A 1S6*
[2]*Department of Chemistry, Baker Laboratory, Cornell University, Ithaca, New York 14853-1301*
(Received 6 May 1996)

In recent experiments, a thin (presumably cylindrical) tubular ''tether'' is mechanically pulled from a roughly spherical fluid-phase lipid-bilayer vesicle. As a first step to understanding these experiments in terms of the commonly used models for vesicle shapes, we examine the mechanical stability of cylindrical vesicle surfaces under axial tension. This should be an adequate description of the extruded tether under the influence of the pulling force, and it provides a starting point for the calculation of the full vesicle shape. It turns out that there is not much difference between an isolated cylindrical vesicle and one where the spherical part of the whole shape is taken into account in an approximate way, giving us reason to believe that our calculation is also relevant to the tether-pulling experiments. Comparison of our results with the experiments shows that the observed tethers fall comfortably within the predicted range of cylindrical stability. [S1063-651X(96)11511-7]

PACS number(s): 82.70.−y, 87.22.Bt, 68.15.+e

I. INTRODUCTION

In recent years, much has been accomplished in the understanding of vesicle shapes. The stationary shapes of freely suspended closed vesicles of spherical topology have been calculated using various models [1,2]. In principle, equilibrium always selects the shape of lowest total energy at given values of the control parameters (vesicle volume V, surface area A, etc.). In practice, two (or more) shapes characterized by the same control parameters may be simultaneously stable, provided that they are both (all) locally stable and that energy barriers are large on the scale of thermal energies k_BT. At true bifurcations or when energy barriers become comparable to k_BT, abrupt shape transformations can occur. Particular attention has been paid to two such shape transformations called budding and vesiculation. A variety of experiments have now provided many examples of locally stable and/or equilibrium shapes and of shape transitions [3].

A particularly simple shape that has attracted some theoretical attention is the cylindrical shape, usually seen experimentally as a tube or ''string'' connected to one or two larger assemblies of membrane material [4]. Theoretical interest here has focused on the stability of free tubes [5,6], on tubes composed of chiral lipids [7], and on a dynamic instability of tubular vesicles induced by perturbing them with a laser beam [8]. In this paper we study static experiments in which a vesicle (or a part of a vesicle) is seen to consist of a tubular segment of membrane under longitudinal tension.

One particular type of experiment exhibiting tubular shapes is that in which a tether is mechanically pulled from a vesicle [9–11]. In these experiments some of the vesicle material (e.g., a swollen red blood cell or a phospholipid vesicle) is sucked into a pipette, forming a ''tongue'' which anchors the vesicle and acts as a reservoir of surface area for the rest of the vesicle. A glass bead is then manipulated so as to touch the vesicle and stick to it. When the bead is subsequently moved away, a long tether is pulled from the vesicle, without significantly perturbing the shape of the remainder of the vesicle. (A schematic picture of the geometry of the experiment is shown in Fig. 1.) The precise structure of such a tether is not known, since in most cases it is so narrow that it is observable optically only as an interference pattern. It is normally assumed that it consists of an ordinary bilayer and that it has a (roughly) cylindrical shape. By observing the amount of material that disappears from the ''tongue'' in the pipette as the tether is drawn out, the radius of the tether can be calculated. Typically, it is of the order of 25 nm [11].

These tether-pulling experiments have heretofore been analyzed in terms of various simplified models [12–14], which assumed stable cylindrical structure, but not until now in the context of the general theoretical shape models referred to above. A calculation has been done to examine the stability of cylindrical tubes [6], but no connection was made with the tether-pulling experiments. It is important to determine whether shapes like this (i.e., a long, narrow cylindrical tube connected to a roughly spherical vesicle) are, in fact,

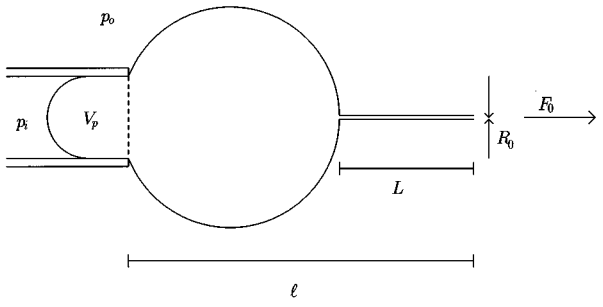

FIG. 1. Sketch of a typical tether-pulling experiment. The vesicle is partially sucked into a pipette, and a tether is pulled out of it in the opposite direction. L is the length of the tether, R_0 is its radius, and F_0 is the pulling force. ℓ is the distance between the mouth of the pipette and the far end of the tether, V_p is the volume of the part of the vesicle that is inside the pipette, p_i is the aspiration pressure inside the pipette, and p_0 is the pressure outside the pipette.

*Present address: Dept. of Chemistry, Baker Laboratory, Cornell University, Ithaca, NY 14853-1301.

consistent with the accepted, modern version [2] of the usual Canham-Helfrich free-energy functional [15]: Otherwise, one would have to conclude either that the theory was wrong or that the actual, microscopic structure of the experimentally observed tether was in some way more complicated, perhaps, e.g., a flattened tube made out of a single leaf of the vesicle bilayer, a bilayer tube that requires additional stabilization by short-range forces across its diameter, or, indeed, a tube with some kind of spatial modulation along its length. It is of particular importance to have a good understanding of the shapes seen in these experiments, because they are commonly used to obtain measurements of the bending moduli κ and $\overline{\kappa}$ of the bilayer [10–13]. From a theoretical point of view, it is convenient that the direction of the force along the cylinder gives the problem axisymmetry, since analytic calculations are limited to axisymmetric shapes.

In order to understand the equilibrium shapes found in the experiments, it is a useful first step to focus on the cylindrical part of the shape and to investigate its stability as a separate unit. Even though the tubular parts of the shapes seen in experiments are not isolated, one would expect them to be close to shapes that are stable by themselves. We shall argue that, in this situation, the remainder of the vesicle can be viewed as a reservoir of surface area and volume for the tube and, thus, can be taken into account in an approximate way, without having to go into the details of the overall shape. We will consider in what follows both isolated cylinders and cylinders connected to such a reservoir. The results for these two different cases will turn out to be the same, thus giving us some confidence that they are valid for a range of cylindrical shapes in different circumstances. To eliminate the effects of the ends of the cylinder, we will consider its length to be much larger than its radius (as is so in the experiments), so that we only study the intrinsic stability of the cylinder itself.

The purpose of this paper is to extend the earlier investigation by Ou-Yang and Helfrich [6] into the stability of cylindrical tubes and to apply it to the tether-pulling experiments discussed above. The extension consists of adding a term representing the force pulling on the tether, as in the experiments, and generalizing the energy functional by including the so-called area-difference-elasticity (ADE) term. In the discussion we will apply the results of the calculation to the experimental situation by substituting representative values for the experimental quantities.

II. THE ENERGY FUNCTIONAL

Our aim is to obtain an energy functional describing the tether (t) which takes into account the rest of the vesicle (r) in an effective, approximate way. We will derive such an expression from the energy functional for the whole vesicle (w), showing along the way what approximations are involved. We assume that the energy of the whole vesicle is described by the area-difference-elasticity (ADE) energy functional [2] plus two additional terms describing an axial pulling force and a pressure difference between the inside and outside of the pipette (Fig. 1)

$$F_w=\frac{\kappa}{2}\int_w dA(C_1+C_2-C_0)^2+\frac{\overline{\kappa\pi}}{2AD^2}(\Delta A-\Delta A_0)^2 - F_0\ell-\Delta p_p V_p . \quad (1)$$

The first term is the Canham-Helfrich curvature energy [15], where κ is the local bending elasticity, C_1 and C_2 are the principal curvatures, and C_0 is the spontaneous curvature. The integral is over the surface of the whole vesicle. The second term is the ADE term, where $\overline{\kappa}$ is the so-called nonlocal bending elasticity, A is the area of the whole vesicle, and D is the distance between the two leaves of the bilayer. ΔA is the total area difference over the entire vesicle between the inner and outer leaves of the bilayer, given by

$$\Delta A=D\int_w dA(C_1+C_2). \quad (2)$$

ΔA_0 is the preferred (''relaxed'') value of this area difference, based on the difference between the number of lipid molecules in the two leaves [2]. The term $-F_0\ell$ represents the effect of the force F_0 (>0) that pulls on the tether; ℓ is the distance from the end of the pipette to the far end of the tether (see Fig. 1). The last term comes from the difference between the aspiration pressure p_i inside the pipette and the pressure p_o outside the pipette, $\Delta p_p=p_o-p_i$ (>0). V_p is the volume of the vesicle tongue inside the pipette. We have omitted from the energy functional the Gaussian curvature term, since the topology of the whole vesicle does not change in the course of the experiment. The surface area and volume of the whole vesicle are regarded as fixed during the experiment.

The integral terms appearing in Eqs. (1) and (2) and the length ℓ can each be written as a sum of two parts, one that depends only on the properties of the tether and another that depends only on the properties of the rest of the vesicle. The full energy (1) can, therefore, be split up in a similar way, except for one term: Expanding the ADE term gives rise to a cross term proportional to $\Delta A_t\Delta A_r$, which depends on the properties of *both* parts (t and r) of the vesicle. In order to decouple completely the two parts of the vesicle (so that we can write $F_w=F_t+F_r$), we shall assume that ΔA_r in this term is constant, i.e., that it does not vary when a small fluctuation is applied to the vesicle shape. One can check that this approximation is good by following Ref. [14] and modeling the rest of the vesicle (r) as a sphere outside the pipette plus a cylindrical tongue inside. Then, a simple model calculation shows that the terms we neglect in taking ΔA_r to be constant here are about five orders of magnitude smaller than the relevant dominant terms. The upshot of this approximation is that the part of the ADE term which refers to the tether can now be written as $(\Delta A-\overline{\Delta A_0})^2$, where $\overline{\Delta A_0}=\Delta A_0-\Delta A_r$ is now the effective preferred area difference for the tether alone (with ΔA_r taken fixed).

Having now written the energy F_w as the sum of two terms that refer separately to the tether and the rest of the vesicle, we introduce one more approximation. The tether and the rest of the vesicle are still connected by the fact that the surface area and volume of the whole vesicle are conserved. So, if the surface area of the tether A_t changes by a small amount δA_t the surface area of the rest of the vesicle changes by $-\delta A_t$ (and similarly for the volume). Since the surface area and volume of the rest of the vesicle are much larger than those of the tether, it effectively forms a reser-

voir, and we expect its energy to change approximately linearly with the changes of surface area and volume (this approximation would break down if there was an unexpected coupling between fluctuation modes in the tether and in the rest of the vesicle). Hence, if we are only interested in fluctuations in the shape of the tether, we can replace the term F_r by two terms that couple to the surface area and volume of the tether, $\Sigma_t A_t - P_t V_t$. The (effective) surface tension and pressure difference are given by $\Sigma_t = \partial F_r/\partial A_t = -\partial F_r/\partial A_r = -\Sigma_r$ and $P_t = -\partial F_r/\partial V_t = \partial F_r/\partial V_r = -P_r$. (A calculation using the same simple model referred to above shows that both Σ_t and P_t defined in this way are positive, as one would expect intuitively.)

The upshot of this is that we can finally write an effective energy functional for the tether alone, taking the rest of the vesicle into account approximately. This functional is given by

$$F = \frac{\kappa}{2}\int dA(C_1+C_2-C_0)^2 + \frac{\overline{\kappa}\,\overline{\pi}}{2\overline{A}\,\overline{D}^2}(\Delta A - \overline{\Delta A_0})^2 - F_0 L + \Sigma A - PV, \tag{3}$$

where we have dropped the subscript t, since, unless otherwise noted, all quantities from now on will refer to the tether. Here, Σ and P are the effective surface tension and pressure difference [16] for the tether (determined by the properties of the reservoir, as discussed in the preceding paragraph); $\overline{A}$ is the surface area of the whole vesicle; $\overline{\Delta A_0}$ is the preferred area difference of the tether; and L is the length of the tether.

Except for the specific interpretations of A, $\overline{\Delta A_0}$, Σ, and P, there is nothing left in the energy functional (3) that refers explicitly to the geometry of the tether-pulling experiment. Therefore, the same functional can be used to describe a vesicle that is in contact with any kind of reservoir, the only difference being the specific values and interpretation of these four parameters. Note that one could interpret Σ and P, not as an effective surface tension and pressure difference, but as Lagrange multipliers used to enforce constraints of constant surface area and volume of the tether. In that case, the description would be appropriate for an isolated cylindrical vesicle. It will turn out that the results for the stability of the cylindrical shape are essentially the same for both these situations, thus showing that the presence of a reservoir of volume and surface area does not influence the stability of the tether shape. This was found earlier for a cylinder without tension [6].

III. STABILITY ANALYSIS

We will now examine the stability against small shape fluctuations of a cylindrical vesicle described by the bending energy (3). The shape of the cylinder with fluctuations can be expanded around a perfect cylinder as

$$\vec{R}(z,\phi) = \vec{R}_0(z,\phi) + \varepsilon(z,\phi)\hat{\vec{n}}_0(z,\phi), \tag{4}$$

where $\vec{R}_0(z,\phi) = (R_0\cos\phi, R_0\sin\phi, z)$ describes an unperturbed cylinder of radius R_0 and $\hat{\vec{n}}_0(z,\phi) = (\cos\phi, \sin\phi, 0)$ is the normal to the surface of that cylinder. The perturbation $\varepsilon(z,\phi)$ may now be expanded as

$$\varepsilon(z,\phi) = \sum_{n,m} \varepsilon_{n,m} e^{i(k_n z + m\phi)}, \tag{5}$$

where $k_n = 2\pi n/L$ and L is the length of the cylinder. z and ϕ run from 0 to L and 0 to 2π, respectively. Since we are interested in the properties of a cylinder which is long compared to its radius, we entirely neglect the shape at the endpoints.

Expanding the surface area, volume, bending energy, and area difference of the shape given by Eq. (4) to order ε^2 and, at the same time, introducing a change of cylinder length, δL, gives

$$\delta A = \delta\left(\int_0^{2\pi} d\phi \int_0^L dz\sqrt{g}\right) = 2\pi L\varepsilon_{0,0} + 2\pi(R_0+\varepsilon_{0,0})\delta L + \frac{\pi L}{R_0}\sum_{n,m}|\varepsilon_{n,m}|^2(k_n^2R_0^2+m^2), \tag{6}$$

$$\delta V = \delta\left(\int_0^{2\pi} d\phi \int_0^L dz \int_0^{R_0} r\,dr\right) = 2\pi L R_0\varepsilon_{0,0} + \pi(R_0^2+2R_0\varepsilon_{0,0})\delta L + \pi L\sum_{n,m}|\varepsilon_{n,m}|^2, \tag{7}$$

$$\delta E = \delta\left(\int_0^{2\pi} d\phi \int_0^L dz (C_1+C_2-C_0)^2\sqrt{g}\right) = -\frac{\kappa\pi L}{R_0^2}(1-R_0^2C_0^2)\varepsilon_{0,0} + \frac{\kappa\pi}{R_0}(1-R_0C_0)^2\delta L - \frac{\kappa\pi}{R_0^2}(1-R_0^2C_0^2)\varepsilon_{0,0}\delta L + \frac{\kappa\pi L}{R_0^3}\sum_{n,m}|\varepsilon_{n,m}|^2 Q_{n,m}, \tag{8}$$

$$\delta\Delta A = \delta\left(D\int_0^{2\pi} d\phi \int_0^L dz (C_1+C_2)\sqrt{g}\right) = 2\pi D\,\delta L + \frac{2\pi L D}{R_0^2}\sum_{n,m}|\varepsilon_{n,m}|^2 k_n^2 R_0^2, \tag{9}$$

where

$$Q_{n,m} = [\tfrac{1}{2}(C_0^2R_0^2-1) - 2C_0R_0](k_n^2R_0^2+m^2) + (k_n^2R_0^2+m^2)^2 + 2(C_0R_0-1)m^2 + 1 \tag{10}$$

and $\sqrt{g}$ is the metric on the surface of the (perturbed) cylinder. Equations (6)–(8) agree with expressions found by Ou-Yang and Helfrich [6], who proceeded by developing general forms for the first and second variations and then specializing to cylindrical geometry.

Substituting all of this into Eq. (3) and expanding the ADE term gives

$$\delta F = \delta^{(1)}F + \delta^{(2)}F + O(\varepsilon^3), \tag{11}$$

with

$$\delta^{(1)}F = \delta L\left\{ \frac{\kappa\pi}{R_0}(1-R_0C_0)^2 + 2\pi R_0\Sigma - \pi R_0^2 P - F_0 + \frac{4\overline{\kappa\pi}^3 L}{\overline{A}}(1-\Delta a_0)\right\} + \varepsilon_{0,0}\left\{ -\frac{\kappa\pi L}{R_0^2}(1-R_0^2C_0^2) + 2\pi L\Sigma - 2\pi L R_0 P\right\}, \tag{12}$$

$$\delta^{(2)}F = \varepsilon_{0,0}\delta L\left\{ -\frac{\kappa\pi}{R_0^2}(1-R_0^2C_0^2) + 2\pi\Sigma - 2\pi R_0 P\right\} + \delta L^2\frac{2\overline{\kappa\pi}^3}{\overline{A}} + \frac{\pi L}{R_0}\sum_{n,m}|\varepsilon_{n,m}|^2 \times\left\{ \frac{\kappa}{R_0^2}Q_{n,m} + (k_n^2R_0^2+m^2)\Sigma - R_0P + \frac{4\overline{\kappa\pi}^2 L}{R_0\overline{A}}(1-\Delta a_0)k_n^2R_0^2\right\}, \tag{13}$$

and where we have defined a reduced version of the preferred area difference, $\Delta a_0 = \overline{\Delta A_0}/2\pi LD$.

The requirement that the first variation of F be zero implies that Σ and P should satisfy

$$P = \frac{F_0}{\pi R_0^2} - \frac{2\kappa}{R_0^3}(1-R_0C_0) - \frac{4\overline{\kappa\pi}^2 L}{\overline{A}R_0^2}(1-\Delta a_0), \tag{14}$$

$$\Sigma = R_0P + \frac{\kappa}{2R_0^2}(1-R_0^2C_0^2). \tag{15}$$

Substituting these expressions into the second variation, Eq. (13), gives

$$\delta^{(2)}F = \frac{\pi L}{R_0}\sum_{n,m}|\varepsilon_{n,m}|^2 B_{n,m} + \delta L^2\frac{2\overline{\kappa\pi}^3}{\overline{A}}, \tag{16}$$

where

$$B_{n,m} = \frac{\kappa}{R_0^2}(k_n^2R_0^2+m^2-1)^2 + \frac{F_0}{\pi R_0}k_n^2R_0^2 + PR_0(m^2-1). \tag{17}$$

This result for $\delta^{(2)}F$ has been derived assuming that Σ and P are an effective surface tension and pressure due to the reservoir, so that the terms $\Sigma A - PV$ are real contributions to the energy, Eq. (3). We will consider below the alternative case, where the surface area and volume of the cylinder are kept fixed.

If we consider F_0, Σ, and P to be given for a certain experimental situation, then the two stationarity equations (14) and (15) determine the radius R_0 and the length L of the tether under those conditions. In the second variation Eq. (16) the coefficient of δL^2, $2\overline{\kappa\pi}^3/\overline{A}$, is clearly positive, so the condition that the cylindrical shape should be locally stable becomes simply that $B_{n,m}\geqslant 0$ for all n, m. In examining $B_{n,m}$ for various values of m, we can consider the number $k_nR_0 = 2\pi nR_0/L$ to be a continuous variable, since $L \gg R_0$. To test stability, then, it will suffice to find the minimum of $B_{n,m}$ for each integer m over the continuous variable k_nR_0 and to examine its sign. This is determined by the values of two scaled parameters, $f = F_0R_0/\kappa\pi$ and $p = PR_0^3/\kappa$. Looking separately at $m=0$, $|m|=1$, and $|m|>1$ reveals that there, indeed, is a region in (f,p)-space where $B_{n,m}\geqslant 0$ for all m and n. This region is shown in Fig. 2. The figure also shows, over the region where the cylindrical shape is not stable, which mode is the most unstable (i.e., which has the most negative value of $B_{n,m}$). Note that the mode with $k_nR_0=0$ and $|m|=1$ has $B_{n,m}=0$ everywhere. This neutral mode corresponds to a translation of the whole cylinder and does not signal a shape instability. Modes with $|m|=1$ and arbitrarily small k_nR_0 have values of $B_{n,m}$ that are arbitrarily close to zero. These modes correspond to bending of the cylinder on longer and longer length scales.

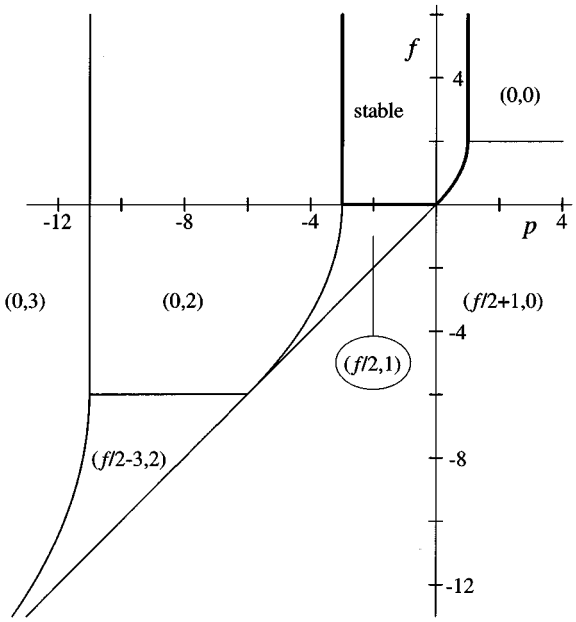

FIG. 2. Plot of scaled (F_0,P) space $(f = F_0R_0/\kappa\pi,\ p = PR_0^3/\kappa)$, showing the region (inside the bold lines) where cylindrical shapes are locally stable, and, for those regions where they are not stable, the values $(k_n^2R_0^2,|m|)$ of the most unstable mode. Further to the right, outside the area of the figure, $m=0$ remains the most unstable mode. Further to the left, there is a succession of bands where modes with consecutively higher values of $|m|$ are the most unstable.

It is useful to comment briefly on the physical significance of the instabilities which bound the region of stability of cylindrical tethers, as illustrated in Fig. 2. This region is bounded below by the horizontal axis, indicating that fluid-membrane tethers are only stable under tension (i.e., $F_0>0$), as is, perhaps, not surprising. What our calculation shows here is that the initial instability that occurs at this boundary is towards a mode with $|m|=1$ and $k_nR_0 = f/2$.

The vertical part of the right-hand boundary of the stable region occurs at $P=\kappa/R_0^3$. When the internal pressure exceeds the external pressure by more than this amount, the tether can lower its energy simply by increasing its radius, i.e., the stationary value R_0 [given implicitly by Eqs. (14) and (15)] becomes a saddle rather than a local energy minimum, as can be verified directly by evaluating the energy (3) for cylindrical geometry. For $0<f<2$, this uniform instability is preempted by one with $k_nR_0=f/2+1$, giving the curved part of the right-hand stability boundary. The left-hand stability boundary occurs for $P=-3\kappa/R_0^3$, i.e., when the external pressure exceeds the internal pressure [16]. The fact that this instability occurs in the sector ($k_nR_0=0$, $m=2$) indicates that the initial collapse of the cylinder is towards a flattened, ribbonlike shape. On the line $F_0=0$, these results are in accordance with earlier work by Ou-Yang and Helfrich [6], who did a similar calculation for the spontaneous curvature model ($\overline{\kappa}=0$) without the pulling force F_0.

If the analogous calculation is done for the alternative case, where the surface area and volume of the cylinder are kept fixed, so that Σ and P are to be interpreted as Lagrange multipliers, almost the same expressions (6)–(17) are recovered. The conditions for making the first variation vanish are, of course, the same, so that Σ and P must again satisfy Eqs. (14) and (15). To find the relevant second variations, some care must be taken: Using the energy functional including the terms $\Sigma A-PV$ would lead to a wrong result. Instead, the constraints on A and V must be taken into account explicitly in the perturbation. The result is again Eq. (16) but without the term $(n,m)=(0,0)$ and the term proportional to δL^2. These two terms correspond, respectively, to variations in the radius and length of the cylinder. Such variations are the only ones that preserve the symmetry of the unperturbed cylindrical shape. It can be shown generally that for perturbations which *break* the symmetry of the unperturbed shape [in this case all $(n,m)\neq(0,0)$], the contribution to the second variation is the same irrespective of whether Σ and P are Lagrange multipliers or the effective (or real) surface tension and pressure difference [17]. The presence or absence of these two terms makes no difference for the stability of the cylinder: The δL^2 term is positive and the term with $(n,m)=(0,0)$ is essentially indistinguishable from the next one, $(n,m)=(1,0)$, since (for large L) k_nR_0 can be considered to be continuously variable. Therefore, the stable area shown in Fig. 2 is valid regardless of whether A or V are kept fixed or, instead, are coupled to a reservoir. This insensitivity to the treatment of the coupling between the tether and the rest of the vesicle reinforces our confidence that the results are valid for the full geometry of the tether-pulling experiments.

An example of an instability in an isolated cylinder is discussed in Ref. [5]. There, it is shown that, for $F_0=0$ and $C_0R_0>1$ (which corresponds here to $P>0$), a modulation along the length of the cylinder develops. It can be shown that the initial wave vector of this modulation, when C_0R_0 first exceeds 1, does, indeed, satisfy $k_nR_0=1$, as would be expected from Fig. 2. Beyond that, shapes develop for which the modulation is no longer infinitesimal, and the present discussion no longer applies.

IV. COMPARISON WITH EXPERIMENTS

Now that we have established the region of cylindrical-tether stability (Fig. 2), it is important to see whether or not the parameters of the tether-pulling experiments [9,11] lie in this region. If they do (which will turn out to be the case), then the previous interpretation of these experiments stands; if they did not, then (assuming the theory to be correct!) the interpretation would have to take into account noncylindrical structures. Such a comparison of theory with the tether experiments can at best be semiquantitative, since many quantities are only roughly known and, indeed, the values found for some quantities depend on the model used to interpret the experiments. On the other hand, as we shall see, it will turn out that the experiments do not fall anywhere near the boundaries of the stability region, so that precise parameter values are not required to verify stability.

The following order-of-magnitude estimates for parameter values seem fairly reliable: $\kappa\approx\overline{\kappa}\approx10^{-19}$ J; $R_0\approx2.5\times10^{-8}$ m; $F_0\approx3\times10^{-11}$ N; $A\approx10^{-9}$ m^2; $L\approx10^{-5}$ – 7×10^{-4} m. The scaled preferred area difference Δa_0 is found to be of order 1 [11], albeit with large fluctuations around that value, particularly if L is small. The difference between the pressure in the pipette and the outside pressure is given in Ref. [11] as $\Delta p_p\approx40$ N/m^2. The effective pressure P can be estimated in the simple model referred to above, and the result is that $P\approx\Delta p_p$. A similar estimate for the effective surface tension gives $\Sigma\approx\Delta p_p\sqrt{A/4\pi}$. We will further assume that the spontaneous curvature is such that $C_0R_0\ll1$, since it seems unlikely that the membrane would have a preference for curvature on a length scale as small as R_0.

Using these parameters, we find that, for short tethers ($L\lesssim5\times10^{-5}$ m), the left-hand side of Eq. (14) and the last term on the right-hand side are negligible compared with the remaining two terms. That equation then reduces to $F_0R_0/\kappa\pi=2$, showing that the radius of the tether is inversely proportional to the pulling force, as was derived before [13] and verified experimentally [9,10]. On the other hand, for long tethers ($L\gtrsim4\times10^{-4}$ m), the ADE term in Eq. (14) is no longer negligible, and the simple inverse proportionality of tether length to pulling force is no longer valid. When this is the case, the effect of the ADE term provides a method to measure both κ and $\overline{\kappa}$, as was done by Waugh *et al.* [11]. An estimate of the surface tension gives $\Sigma\approx10^{-4}$ N/m, which agrees with Eq. (15) and is the same order of magnitude as the (effective) tension mentioned in the literature [9]. Finally, we note that $f=F_0R_0/\kappa\pi\approx2$, and $p=PR_0^3/\kappa\approx10^{-2}$. Thus the axial tension is positive and the dimensionless pressure difference is small, so the observed tethers fall comfortably inside the expected region of (local) cylindrical stability shown in Fig. 2.

We conclude from the above analysis that the tethers observed in tether-pulling experiments [9–11] may consistently be interpreted within the ADE model [2] as locally stable, cylindrical objects, without invoking any additional (e.g., short-range) forces. It seems likely that the full vesicle shape (see Fig. 1) can also be understood within this context, but this proposition remains to be tested (and it would, of course, be necessary to include the forces of constraint where the tongue is sucked into the pipette). Note that the distinction

between the behavior of short and long tethers, which was observed and analyzed in Ref. [14], is a result of a competition between the ADE term in Eq. (3) and the local-bending (Canham-Helfrich) term. Indeed, it is precisely this competition which allows separate measurement of κ and $\bar{\kappa}$ in the tether-pulling experiments; conversely, the consistency of the experiments is a test of the ADE model. Finally, we remark that it has recently become possible to manipulate these phospholipid tethers in the lab to produce nanoscale ''microplumbing'' and to build what is effectively a pico-Newton force balance [18]. A quantitative theoretical understanding of the tethers and the way they connect to the rest of the vesicle allows the axial force on the tether (which is too small to be resolvable optically) to be inferred from the deformation of the remainder of the vesicle, which is large enough to be visible.

ACKNOWLEDGMENTS

D.J.B. is grateful to Dr. Ling Miao for useful and stimulating discussions. This work was supported in part by the Natural Sciences and Engineering Research Council of Canada. Part of it was carried out in the research group of B. Widom, with support from the National Science Foundation and the Cornell University Materials Science Center.

[1] H.J. Deuling and W. Helfrich, J. Phys. (Paris) **37**, 1335 (1976); S. Svetina and B. Žekš, Eur. Biophys. J. **17**, 101 (1989); L. Miao, B. Fourcade, M. Rao, M. Wortis, and R.K.P. Zia, Phys. Rev. A **43**, 6843 (1991); U. Seifert, K. Berndl, and R. Lipowsky, *ibid.* **44**, 1182 (1991).

[2] L. Miao, U. Seifert, M. Wortis, and H.-G. Döbereiner, Phys. Rev. E **49**, 5389 (1994).

[3] E.A. Evans and W. Rawicz, Phys. Rev. Lett. **64**, 2094 (1990); K. Berndl, J. Käs, R. Lipowsky, E. Sackmann, and U. Seifert, Europhys. Lett. **13**, 659 (1990); J. Käs and E. Sackmann, Biophys. J. **60**, 825 (1991); P. Méléard, J.F. Faucon, M.D. Mitov, and P. Bothorel, Europhys. Lett. **19**, 267 (1992); H.-G. Döbereiner, J. Käs, D. Noppl, J. Sprenger, and E. Sackmann, Biophys. J. **65**, 1396 (1993).

[4] M. Bessis, *Living Blood Cells and their Ultrastructure* (Springer, Berlin, 1973), pp. 61, 170; R.M. Servuss, W. Harbich, and W. Helfrich, Biochim. Biophys. Acta **436**, 900 (1976); R. Bar-Ziv and E. Moses, Phys. Rev. Lett. **73**, 1392 (1994). See also Refs. [9,11].

[5] H.J. Deuling and W. Helfrich, Blood Cells **3**, 713 (1977).

[6] Z.-C. Ou-Yang and W. Helfrich, Phys. Rev. A **39**, 5280 (1989).

[7] J.V. Selinger and J.M. Schnur, Phys. Rev. Lett. **71**, 4091 (1993).

[8] P. Nelson, T. Powers, and U. Seifert, Phys. Rev. Lett. **74**, 3384 (1995).

[9] R.M. Hochmuth, H.C. Wiles, E.A. Evans, and J.T. McCown, Biophys. J. **39**, 83 (1982).

[10] L. Bo and R.E. Waugh, Biophys. J. **55**, 509 (1989).

[11] R.E. Waugh, J. Song, S. Svetina, and B. Žekš, Biophys. J. **61**, 974 (1992).

[12] R.M. Hochmuth and E.A. Evans, Biophys. J. **39**, 71 (1982).

[13] R.E. Waugh and R.M. Hochmuth, Biophys. J. **52**, 391 (1987).

[14] B. Božič, S. Svetina, B. Žekš, and R.E. Waugh, Biophys. J. **61**, 963 (1992).

[15] P.B. Canham, J. Theor. Biol. **26**, 61 (1970); W. Helfrich, Z. Naturforsch. **C28**, 693 (1973).

[16] Note that, in the actual tether-pulling experiments, the excess pressure P inside the tether is intrinsically positive. We will for completeness study the stability problem for both signs of P. Only $P>0$ (i.e., the right-hand side of Fig. 2) is relevant to the experiments.

[17] U. Seifert, Z. Phys. B **97**, 299 (1995).

[18] E. Evans (private communication).